High-Frequency Vibration Sensor Using a Fiber Laser With a Multicore Fiber Interferometer

Angel I. Correa, Marko Galarza, Romain Dauliat, Raphael Jamier, Philippe Roy, Manuel Lopez-Amo, *Senior Member, IEEE*, and Rosa A. Perez-Herrera

***Abstract*—We present an interferometric vibration sensor that uses three-core fibers. The transducer is constructed by splicing a segment 20 mm long of a multicore optical fiber (MCF) to a single-mode optical fiber (SMF). The end of the MCF segment is cut off and painted using silver metallic paint. The sensor head is operated in reflection mode. The structure is placed on a polyvinyl chloride (PVC) plate, which is excited with a wide range of frequency signals. The vibrations induce cyclic bending in the MCF segment, resulting in periodic oscillations of the reflected interference spectrum. This device is demonstrated to be suitable to measure vibrations in a frequency range of the order of 300 kHz detecting deformations as small as 0.40 μm.**

***Index Terms*—Interferometer, multicore optical fiber, vibration.**

I. Introduction

VIBRATION analysis plays an essential role in ultrasonic medical diagnostics [1]. In the automotive industry, vibrations are studied to evaluate components such as bearings and exhaust systems [2]. It is a complex process involving the evaluation of a wide variety of frequency ranges [3]. This complexity is closely related to both the inherent structure and the most relevant vibration modes [4], [5]. Given the many applications and broad spectrum of interest, a wide variety of sensors (also called accelerometers) have been developed.

The use of optical fibers to monitor vibrations offers several significant advantages, such as their immunity to electromagnetic interference and corrosion, their long-distance interrogation capability, and their inherent flexibility, among others [6]. These advantages have driven the optical fiber-based vibration sensors to a high development level [7], [8].

Manuscript received 6 November 2023; revised 22 December 2023; accepted 22 December 2023. Date of publication 17 January 2024; date of current version 14 March 2024. This work was supported in part by projects PID2019-107270RB-C02 and PID2022-137269OB-C21, funded by MCIN/AEI/10.13039/501100011033 and FEDER "A way to make Europe," and TED2021-130378B-C22 funded by MCIN/AEI/10.13039/501100011033 and European Union "Next generation EU"/PRTR. The associate editor coordinating the review of this article and approving it for publication was Prof. Santosh Kumar. *(Corresponding author: Angel I. Correa.)*

Angel I. Correa, Marko Galarza, Manuel Lopez-Amo, and Rosa A. Perez-Herrera are with the Department of Electrical, Electronic and Communication Engineering and the Institute of Smart Cities (ISC), Public University of Navarra, 31006 Pamplona, Spain (e-mail: angelignacio.correa@unavarra.es; marko.galarza@unavarra.es; mla@unavarra.es; rosa.perez@unavarra.es).

Romain Dauliat, Raphael Jamier, and Philippe Roy are with the Department of Fiber Photonics, UMR CNRS/University of 7252 Limoges 87060 Limoges, France (e-mail: romain.dauliat@xlim.fr; raphael.jamier@xlim.fr; philippe.roy@xlim.fr).

Digital Object Identifier 10.1109/JSEN.2023.3348502

There are several approaches to detect vibrations using optical fibers, such as Fabry–Pérot interferometers, fiber Bragg gratings (FBGs) [7], [9], and multicore fiber (MCF) interferometers [10], [11]. The design of MCF fibers can be classified as weakly and strongly coupled. In the first case, the cores are typically far apart, reducing the coupling between them and increasing the mode beating length. The second group instead leads us to a stronger coupling and shorter beating lengths.

Given the maturity reached by the Bragg grating technology, many sensors combine FBGs inscribed over weakly coupled multicore fibers [12], [13]. The usual applications of such sensors are to monitor curvature, bending, or shape [2], [10]. Their main advantage is their ability to distinguish the direction of curvature to achieve 3-D shape detection with a single MCF. However, a disadvantage of MCF cores containing Bragg gratings is the need for expensive input–output coupling devices to interrogate each core individually.

With a similar approach, some MCF-based vibration sensors have been reported in recent years. Table I presents a review of interferometer-based vibration sensors. The results indicate that the interferometric vibration sensors based on MCF can provide a wide frequency measurement range, ranging from 1 mHz [14] to 12 kHz [15]. The maximum experimentally measured frequency is 12 kHz, while the maximum theoretically measured frequency is 25 kHz.

In the present work, a high-frequency vibration sensor based on an MCF fiber operating in reflection mode is presented.

Our sensor design is based on a reflection mode structure. This structure acts as an interferometric sensor because of the interference of the even super-modes of the three-core waveguide. It also acts as one of the mirrors of an optical fiber laser. By painting the end of the multicore fiber structure, a mirror is created, providing an average reflectivity of 86.8% [24].

TABLE I
MCF INTERFEROMETER-BASED VIBRATION SENSORS

Range	Sensor Structure	Applications	Year / Ref.
1 mHz–30 Hz/0.76 mg–29.64 mg (acceleration)	Phase-shifted modal interferometers	Accelerometers	2020 [14]
1–20 Hz	Three-core fiber SMI*	Long-term monitoring of construction and mechanical structures	2019 [16]
5–50 Hz/0.00 g–0.04 g (acceleration)	Seven-core fiber SMI	Low-frequency accelerometers	2018 [17]
5–100 Hz	Three-core fiber SMI	Low-frequency and low-amplitude seismic sensing	2018 [18]
30–240 Hz	Packaged seven-core fiber SMI	Low-frequency vibration sensing	2018 [10]
60–290 Hz	Seven-core fiber SMI	Commercial vibration sensing applications	2017 [11]
Below 500 Hz	Dual-core fiber MI	Accelerometers	2011 [20]
40–760 Hz in experiment and 50 Hz–25 KHz in theory	Seven-core fiber SMI	Diverse vibration sensing applications	2017 [21]
1–1050 Hz	Phase-shifted modal interferometers	Various vibration measurements	2019 [22]
2–2500 Hz	Seven-core fiber SMI	A variety of practical applications	2017 [23]
1 kHz–12 kHz	MI* composed of seven-core fan-in coupler	Long-distance vibration measurement	2018 [15]

* Michelson interferometer (MI); Supermode interferometer (SMI).

It increases the reflectivity and, consequently, the amplitude of the reflected transfer function. Thus, sensitivity is increased, and because the propagation path is doubled, the final length of the interferometer involves several coupling lengths to achieve a good sensitivity. This configuration doubles the sensing length of the interferometer and uses a single fiber for the input–output connection, making it easier to place in real assemblies.

The construction was carried out by splicing a few millimeters of the MCF fiber to a standard single-mode optical fiber and placing a standard metallic paint-based high reflectivity mirror at the other fiber end. The structure was fixed to the end of a polyvinyl chloride (PVC) plate from Sentra, which was vibrated using a mechanical waveform controller. The sensor structure was placed as a mirror of an erbium-doped fiber laser linear cavity, whose signal was converted to the electrical domain and processed to determine the vibration frequency.

II. SENSOR DESIGN

As mentioned, the multicore fibers used for the development of these interferometers consist of three cores. Fig. 1 shows schematics and microscope photographs of the cross sections of the fibers. The MCF fiber depicted in Fig. 1(a) presents a fiber with in-line arrangement with core-to-core separations of 9.92 and 11.03 μm and a central core diameter of 9.09 μm. Fig. 1(c) shows the fiber with a V-arrangement whose cores are separated 10.49 and 10.29 μm and whose central core diameter is 9.18 μm. The microscope photographs in Fig. 1(b) and (d) have been taken with the FIP-400B connector inspector.

A fully vectorial finite difference mode solver has been used for the analysis of the multicore fibers. Fig. 2 shows the symmetric field distribution of the fundamental and second-order LP_{01} supermodes for both in-line and V arrangements. The first-order asymmetric mode is omitted because the mode

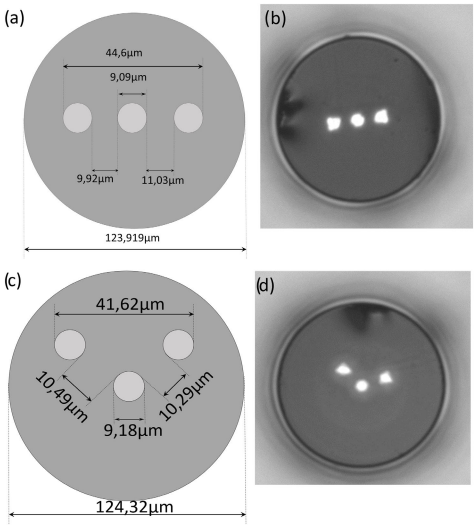

Fig. 1. Cross-sectional diagrams for (a) in-line three-core and (c) in-V three-core fibers. Fiber cross sections taken with FIP-400B fibers inspection probe for (b) in-line three-core and (d) in-V three-core fibers.

of the SMF fiber does not excite it. In fact, the symmetric supermodes carry nearly all the power, with 54% for the fundamental mode and 46% for the second-order mode. The propagation analysis shown in Fig. 3 over 40 mm provides a beat length or around 18 mm for the in-line multicore configuration and 30 mm for the V arrangement.

Using a high-resolution optical backscatter reflectometer (LUNA OBR 4600), we conducted an analysis of the reflected power from both in-line and in V structures, obtaining the reflection spectrum for lengths of 30 and 50 cm, respectively. Fig. 4(a) shows the central core's power coupling in and out to the sides six times every 10 cm, to provide an estimated coupling length of 16 mm. The same phenomenon can be observed in Fig. 4(b) for the V arrangement, where the coupling length

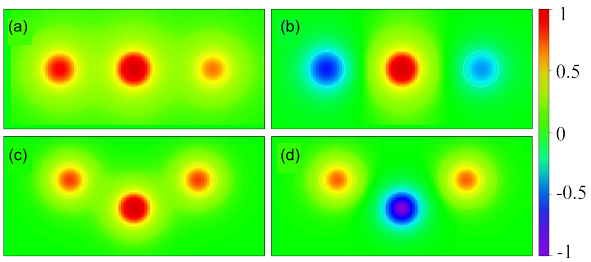

Fig. 2. Normalized field distribution of (a) fundamental and (b) second-order supermodes of the in-line multicore structure. (c) and (d) Supermodes for the V arrangement.

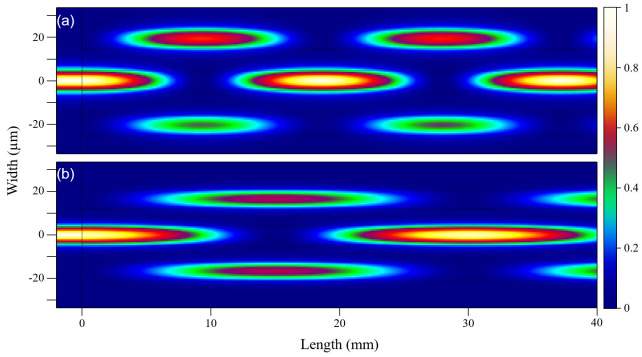

Fig. 3. Intensity distribution along 40 mm in (a) in-line and (b) V-arrangement multicore fibers excited by a standard single-mode fiber.

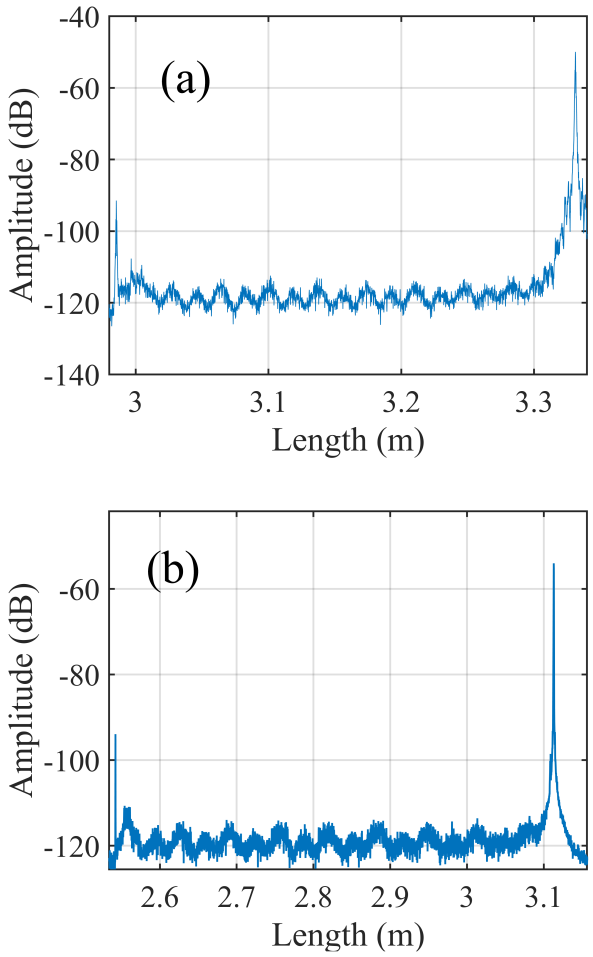

Fig. 4. Backscattered optical power as a function of fiber length from (a) three-core in-line fiber, 30 cm and (b) three-core in-V fiber, 50 cm fiber. Measurements carried out using an OBR (4600 from Luna).

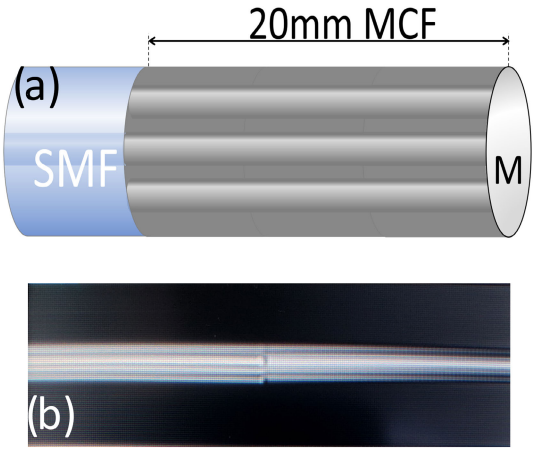

Fig. 5. (a) Sensor structure: single-mode fiber (SMF), multicore fiber (MCF), and mirror (M). (b) Photograph of the MCF sensor taken using a Fujikura 100P fiber fusion splicer.

is approximately 28 mm. Both results are in good agreement with the theoretical calculations.

The sensor fabrication was carried out by splicing a 20-mm segment of three-core MCF to a single-mode fiber, as shown in Fig. 5(a). A silver-painted mirror was applied at the right end of the MCF segment (indicated as M). A Fujikura FSM-100p+ fusion splicer was used to splice both elements. Fig. 5(b) shows a photograph of the fusion between the MCF and SMF segment, captured using the built-in fusion splicer's microscope. During the manufacturing process, a very efficient coupling between the SMF and the MCF was achieved, resulting in a low insertion loss. By carefully adjusting the splicing process, we achieve losses as low as 0.01 dB.

In our design, the sensor was placed on the edge of a PVC plate, exposed to the controlled motion of a Mechanical Wave Controller SF-9324. It was excited with a sine wave provided by an HP33120A signal generator. The vibration was measured with an electronic commercial sensor (LDT1-028K), placed under the PVC sheet, and taken as a reference, as presented in Fig. 6. The photograph shows the experimental setup of the sensor.

As the PVC plate vibrates, it exerts forces on the multicore fiber, causing it to bend cyclically. This bending introduces periodic variations in the fiber's physical structure. When the fiber bends due to the vibrations, it alters the optical path lengths of these cores, affecting the interference patterns.

The vibration causes periodic deformation in the MCF, leading to cyclic changes in the modes of interference and, consequently, periodic changes in the interference pattern [9], [25], [26], [27].

The setup in Fig. 7 was used to obtain the interference pattern of the structure. A broadband light source (BLS) was injected into the circulator at port 1. The SMF-MCF structure

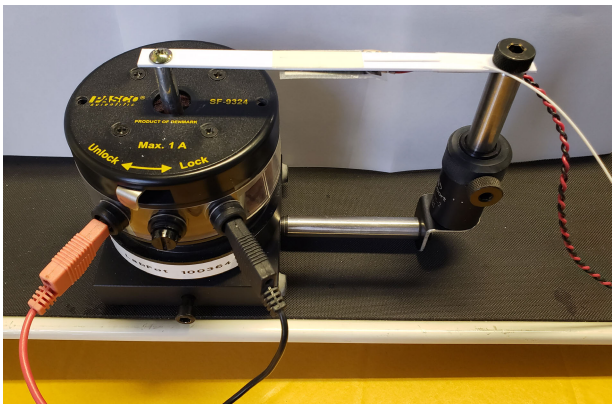

Fig. 6. Experimental setup of the sensor to apply the vibration frequency.

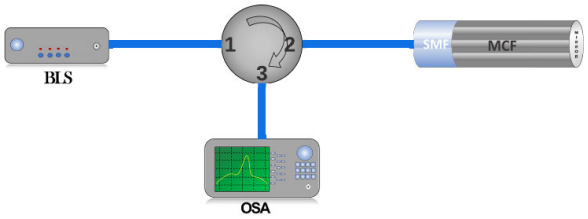

Fig. 7. Experimental setup for the measurement of the interference pattern in reflection.

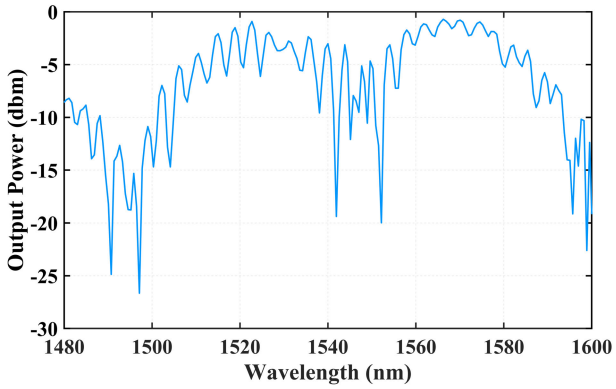

Fig. 8. Reflected optical spectrum of the 20-mm MCF segment measured using an OSA.

was connected to port 2, and the reflected signal was measured with an optical spectrum analyzer (OSA) connected to port 3 of the circulator.

The resulting optical spectrum response measured by the 0.1-nm resolution OSA and showing the interference pattern is depicted in Fig. 8.

III. Experimental Setup

To interrogate the sensor, the erbium-doped linear fiber laser shown in Fig. 9 was arranged. This structure has already exhibited excellent performance in sensing, as it was reported in [28]. A 980-nm pumping laser is injected into the linear-cavity fiber laser via the 980-/1550-nm wavelength-division multiplexer (WDM). The gain medium, located at the 1550-nm port of the WDM, consists of 3.4 m of erbium-doped fiber (EDF). This EDF used is type I25 (980/125), ideal

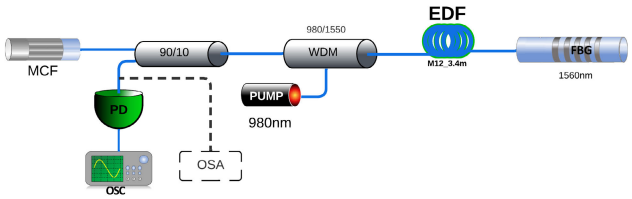

Fig. 9. Experimental setup of the sensor head in the linear-cavity laser.

for its use in C-band amplifiers and with a core composition optimized for EDF amplifiers (EDFAs) in dense wavelength-division multiplexing (DWDM) network systems. The maximum core absorption ranges from 7.7 to 9.4 dB/m at 1531 nm. The linear cavity of the laser terminates at an FBG, which acts as a filter to reflect the 1560-nm wavelength.

The filtered signal traverses the 1500-nm port of the WDM to reach the optical coupler where 10% of the signal is directed to the OSA and the remaining 90% is injected into the MCF structure.

The photodetector converts the optical signal into an electrical signal for subsequent analysis with an oscilloscope. The system was isolated from external vibrations for the experimental measurement, and temperature compensation was not implemented.

The sensor's characterization was developed at a stable room temperature of 21 °C. If the operating temperature of the vibration sensor is expected to change during its operation, temperature compensation can be implemented. To achieve a complete optical solution, we can use the Bragg grating (FBG) present in the experimental setup, which works as a mirror of the laser structure. To measure the wavelength shift of the laser caused by temperature variation in the FBG, it is enough to take a low-frequency measurement using an OSA [29].

IV. Experimental Results

Fig. 10 shows the optical output spectrum measured with the OSA for the linear-cavity configuration, including the MCF structure. A laser peak centered at 1560 nm with an output power level of −3.36 dBm and an optical signal-to-noise ratio (OSNR) of 24.52 dB was obtained when pumped with 71.53 mW.

The photodetected signal is processed by using the fast Fourier transform (FFT) to calculate the vibration frequency. The obtained results are validated by means of the commercial electronic vibration sensor LDT1-028K from Thorlabs. Fig. 11 shows the frequency response for an excitation frequency of 15 kHz measured with the electronic sensor.

On the other hand, Fig. 12(a) and (b) shows the response obtained using the proposed cavity for two 20-mm fiber fragments with different core distribution patterns (in-line and V, respectively) and for an excitation signal of 15 kHz. It can be observed that the measured spectral response follows the mechanical excitation.

The signal measured with the electronic sensor is used as a reference for subsequent measurements, in which a frequency sweep is performed for a better and more accurate characterization of the sensor. The sweep range is established

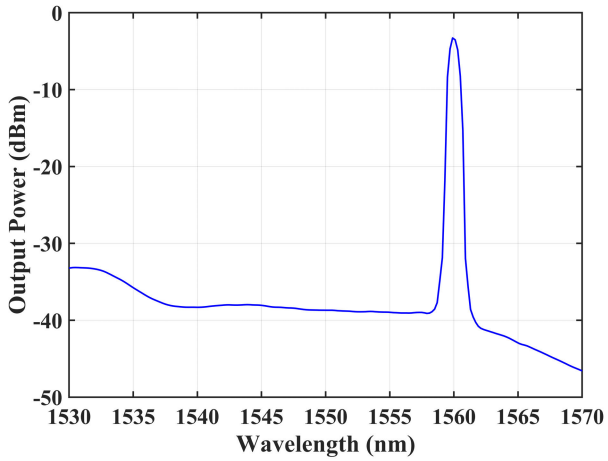

Fig. 10. Output spectrum measured with the OSA for the linear-cavity laser configuration, including the MCF sensor head.

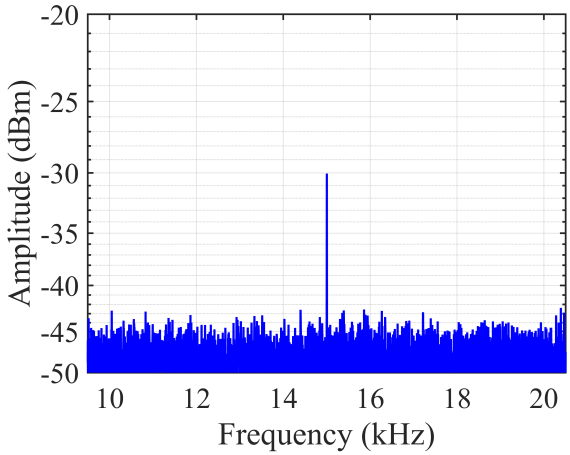

Fig. 11. Frequency response of an electronic commercial sensor, excited with a 15-kHz vibration.

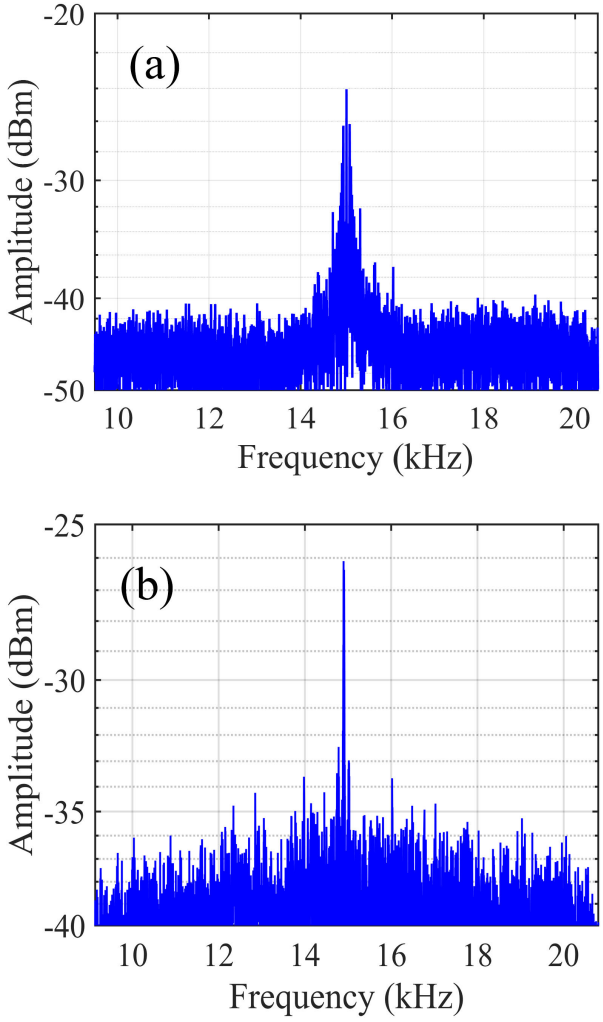

Fig. 12. Frequency response for a 20-mm-long fiber sensor head. (a) Three cores in-line. (b) Three cores in V for an excitation signal of 15 kHz.

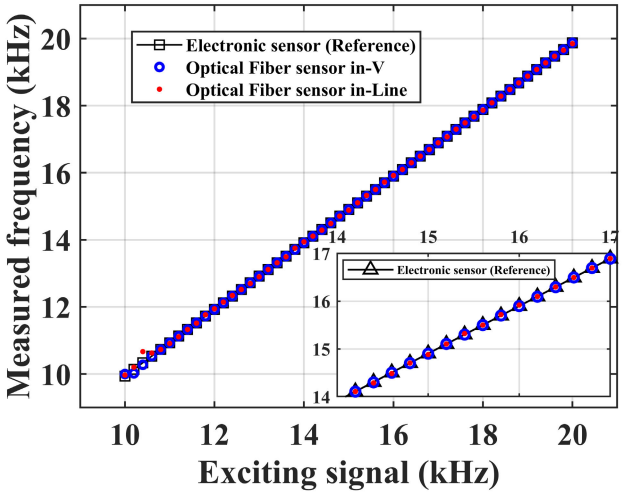

Fig. 13. Excitation signal versus measured signal, the inset graph shows a close-up of the measured points.

from 10 to 20 kHz with steps of 100 Hz, resulting in the graph shown in Fig. 13. The inset figure amplifies the range between 14 and 17 kHz in which the measurement has a clear linear trend. It is observed that the frequency response of the sensors for the measured range shows a high linearity. The calculated, coefficient of determination (R^2) for the signals measured with both sensors is very close to 1.

In the second stage of the evaluation process of the fabricated sensors, the setup shown in Fig. 14 was used to excite the sensor in a higher frequency range. It is composed of a piezoelectric PZT shear chip PL5FBP3 that provides a maximum lateral displacement of 1.3 μm $\pm$ 20% when driven from -200 to $+200$ V. The operation voltage range used for this configuration is ± 127 V, achieving a displacement of approximately 30% of the maximum range.

Measuring the setup described in Fig. 9 to interrogate the sensor head, PL5FBP3 was exited with frequencies in the range of 80–179 kHz. The response of the proposed SMF-MCF structure for both in-line and in-V distributions is shown in Fig. 15. The spectra shown in this figure demonstrate that the structure can accurately measure high frequencies with vibration amplitudes as low as 0.40 μm.

Fig. 16 depicts the recorded data for the whole frequency range, measured with a frequency gap of 1 kHz. The inset shows a portion of the spectrum ranging from 130 to 150 kHz

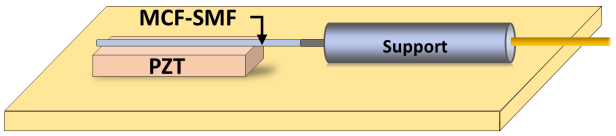

Fig. 14. Experimental setup of the sensing head to apply the vibration frequency of 50–300 kHz using a PL5FBP3 piezoelectric controller.

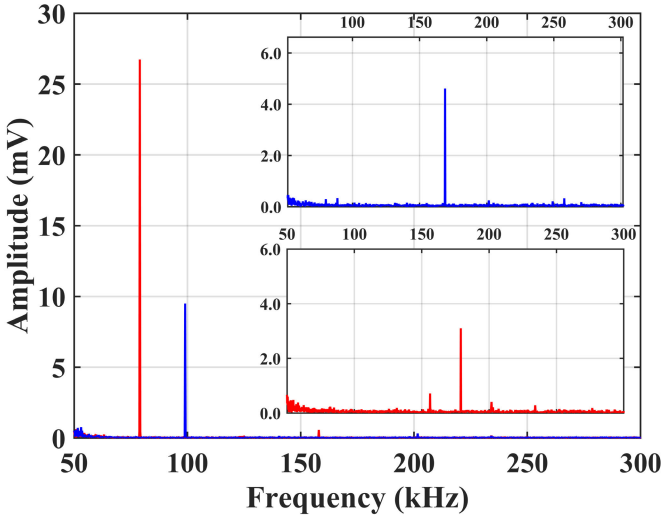

Fig. 15. Frequency response for three-core in-line (red) and three-core in-V (blue) fiber-based sensor head for a 50–300-kHz frequency sweep.

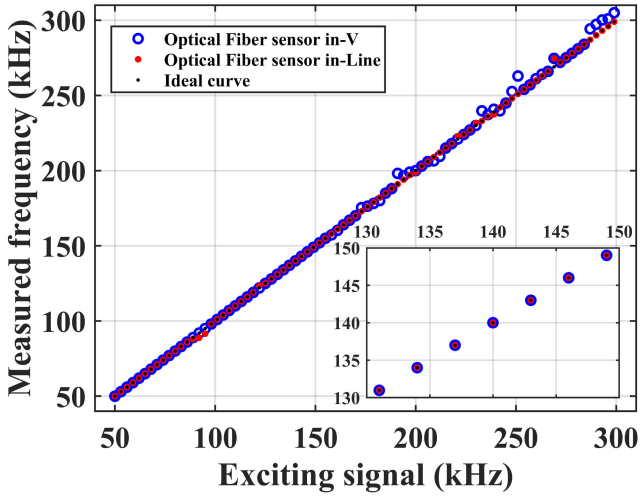

Fig. 16. Excitation signal versus measured signal for both sensing heads.

in which the excitatory signal points versus measured frequency present a linear tendency.

V. Conclusion

A vibration sensor has been developed by splicing a short segment of a three-core fiber with a standard single-mode fiber and applying a metallic paint layer at the end of the multicore fiber to achieve high reflectivity. The sensor's manufacturing was carried out using tools and processes standard in the telecommunications industry, which becomes a cost-effective solution. In order to achieve a good OSNR in measurements, we have implemented a fiber laser sensing structure, where the three-core fiber transducers act as a mirror of this laser.

It has been demonstrated that this MCF-based interferometric sensor head is highly accurate and reliable for monitoring vibrations in the range of 10–300 kHz. The obtained data were compared with those from a reference electronic sensor and the high correlation between both sensors was confirmed, resulting in $R^2 = 0.99$. These results surpass the records reported in [16], where a three-core fiber-based sensor was implemented in the frequency range of up to 20 Hz. This new-type MCF-SMF interferometric sensor can accurately measure vibrations in the high-frequency range.

Acknowledgment

The authors would like to thank Armando Rodriguez for his help in measurements and useful discussions. Open Access funding provided by Universidad Pública de Navarra.

References

[1] C. T. Leondes, *MEMS/NEMS: Handbook Techniques and Applications*. New York, NY, USA: Springer, 2006.

[2] R. B. Randall, *Vibration-Based Condition Monitoring: Industrial, Automotive and Aerospace Applications*, 2nd ed. Hoboken, NJ, USA: Wiley, 2022.

[3] R. Soman, J. Wee, and K. Peters, "Optical fiber sensors for ultrasonic structural health monitoring: A review," *Sensors*, vol. 21, no. 21, p. 7345, Nov. 2021, doi: 10.3390/s21217345.

[4] M. D. Caicedo, "Períodos de vibración de las edificaciones.," *Revista de Arquitectura e Ingeniería*, vol. 8, no. 2, pp. 1–13, 2014.

[5] V. V. Silberschmidt, *Dynamic Deformation, Damage and Fracture in Composite Materials and Structures*. Amsterdam, The Netherlands: Elsevier, 2023, doi: 10.1016/C2020-0-01086-8.

[6] D. A. Krohn, *Fiber Optic Sensors: Fundamentals and Applications*, 4th ed. Bellingham, WA, USA: SPIE Press, 2014.

[7] Y. R. García, J. M. Corres, and J. Goicoechea, "Vibration detection using optical fiber sensors," *J. Sensors*, vol. 2010, pp. 1–12, Jul. 2010, doi: 10.1155/2010/936487.

[8] M. Morante, "New approach using a bare fiber optic cantilever beam as a low-frequency acceleration measuring element," *Opt. Eng.*, vol. 35, no. 6, p. 1700, Jun. 1996, doi: 10.1117/1.600745.

[9] Y. Yao, Z. Zhao, and M. Tang, "Advances in multicore fiber interferometric sensors," *Sensors*, vol. 23, no. 7, p. 3436, Mar. 2023, doi: 10.3390/s23073436.

[10] J. Villatoro et al., "Packaged multi-core fiber interferometric vibration sensor," in *Conf. Lasers Electro-Opt., OSA Tech. Dig.* Optica Publishing Group, 2018, Paper SM2K.6, doi: 10.1364/CLEO_SI.2018.SM2K.6.

[11] J. Villatoro, O. Arrizabalaga, E. Antonio-Lopez, J. Zubia, and I. S. de Ocáriz, "Multicore fiber sensors," in *Opt. Fiber Commun. Conf., OSA Tech. Dig.* Optica Publishing Group, 2017, Paper Th3H.1, doi: 10.1364/OFC.2017.Th3H.1.

[12] H. Zhang et al., "Fiber Bragg gratings in heterogeneous multicore fiber for directional bending sensing," *J. Opt.*, vol. 18, no. 8, Aug. 2016, Art. no. 085705, doi: 10.1088/2040-8978/18/8/085705.

[13] G. M. H. Flockhart, W. N. MacPherson, J. S. Barton, J. D. C. Jones, L. Zhang, and I. Bennion, "Two-axis bend measurement with Bragg gratings in multicore optical fiber," *Opt. Lett.*, vol. 28, no. 6, p. 387, Mar. 2003, doi: 10.1364/OL.28.000387.

[14] J. Amorebieta et al., "Highly sensitive multicore fiber accelerometer for low frequency vibration sensing," *Sci. Rep.*, vol. 10, no. 1, p. 16180, Sep. 2020, doi: 10.1038/s41598-020-73178-x.

[15] Z. Zhao et al., "Robust in-fiber spatial interferometer using multicore fiber for vibration detection," *Opt. Exp.*, vol. 26, no. 23, p. 29629, Nov. 2018, doi: 10.1364/OE.26.029629.

[16] L. Cai, J. Pan, P. Yue, and N. Zhong, "Theoretical analysis and application of MTM fiber structure based low-frequency vibration sensor," *Optik*, vol. 195, Oct. 2019, Art. no. 163161, doi: 10.1016/j.ijleo.2019.163161.

[17] J. Villatoro et al., "Simple multi-core optical fiber accelerometer," in *Adv. Photon. (BGPP, IPR, NP, NOMA, Sensors, Netw., SPPCom, SOF), OSA Tech. Dig.* Optica Publishing Group, 2018, Paper SeW3E.4, doi: 10.1364/SENSORS.2018.SeW3E.4.

[18] J. Villatoro, A. Ortega-Gomez, J. Zubia, E. Antonio-Lopez, A. Schülzgen, and R. Amezcua-Correa, "Ultrasensitive vibration sensor based on an asymmetric multi-core optical fiber," in *26th Int. Conf. Opt. Fiber Sensors, OSA Tech. Dig.* Optica Publishing Group, 2018, Paper ThE68, doi: 10.1364/OFS.2018.ThE68.

[19] B. Gökbulut and M. N. Inci, "An interferometric vibration sensor based on a four-core optical fiber," *Proc. SPIE*, vol. 9899, Apr. 2016, Art. no. 989920, doi: 10.1117/12.2225897.

[20] F. Peng et al., "In-fiber integrated accelerometer," *Opt. Lett.*, vol. 36, no. 11, p. 2056, Jun. 2011, doi: 10.1364/OL.36.002056.

[21] J. Villatoro, E. Antonio-Lopez, A. Schülzgen, and R. Amezcua-Correa, "Miniature multicore optical fiber vibration sensor," *Opt. Lett.*, vol. 42, no. 10, p. 2022, May 2017, doi: 10.1364/OL.42.002022.

[22] J. Villatoro, "Phase-shifted modal interferometers for high-accuracy optical fiber sensing," *Opt. Lett.*, vol. 45, no. 1, p. 21, Jan. 2020, doi: 10.1364/OL.45.000021.

[23] J. Villatoro, E. Antonio-Lopez, J. Zubia, A. Schülzgen, and R. Amezcua-Correa, "Interferometer based on strongly coupled multi-core optical fiber for accurate vibration sensing," *Opt. Exp.*, vol. 25, no. 21, p. 25734, Oct. 2017, doi: 10.1364/OE.25.025734.

[24] I. Jaso, E. Mejia-Olivo, M. B. Acha, D. Leandro, and M. Lopez-Amo, "Fiber optic mirror fabrication using general-purpose metallic pigments," in *Proc. Eur. Workshop Opt. Fibre Sensors (EWOFS)*, M. Wuilpart and C. Caucheteur, Eds., Mons, Belgium: SPIE, May 2023, p. 126, doi: 10.1117/12.2681210.

[25] A. M. Ortiz and R. L. Sáez, "Multi-core optical fibers: Theory, applications and opportunities," in *Selected Topics on Optical Fiber Technologies and Applications*, F. Xu and C. Mou, Eds. Rijeka, Croatia: InTech, 2018, doi: 10.5772/intechopen.72458.

[26] J. E. Antonio-Lopez, Z. S. Eznaveh, P. LiKamWa, A. Schülzgen, and R. Amezcua-Correa, "Multicore fiber sensor for high-temperature applications up to 1000°C," *Opt. Lett.*, vol. 39, no. 15, p. 4309, Aug. 2014, doi: 10.1364/OL.39.004309.

[27] A. V. Newkirk, J. E. Antonio-Lopez, A. Velazquez-Benitez, J. Albert, R. Amezcua-Correa, and A. Schülzgen, "Bending sensor combining multicore fiber with a mode-selective photonic lantern," *Opt. Lett.*, vol. 40, no. 22, pp. 5188–5191, Nov. 2015, doi: 10.1364/OL.40.005188.

[28] R. A. Perez-Herrera, D. Pallarés-Aldeiturriaga, A. Júdez, L. Rodriguez Cobo, M. Lopez-Amo, and J. M. Lopez-Higuera, "Optical fiber lasers assisted by microdrilled optical fiber tapers," *Opt. Lett.*, vol. 44, no. 11, p. 2669, Jun. 2019, doi: 10.1364/OL.44.002669.

[29] X. Wang, X. Sun, Y. Hu, L. Zeng, Q. Liu, and J. Duan, "Highly-sensitive fiber Bragg grating temperature sensors with metallic coatings," *Optik*, vol. 262, Jul. 2022, Art. no. 169337, doi: 10.1016/j.ijleo.2022.169337.